Energy Reports 8 (2022) 13484–13493

Contents lists available at ScienceDirect

Energy Reports

journal homepage: www.elsevier.com/locate/egyr

Research paper

Analysis and implementation of a solar/biogas hybrid system for centralized generation at Qadirpur Ran

Muhammad Imran [a], Zeeshan Rashid [b], Muhammad Amjad [c], Shadi Khan Baloch [d], Adil Mustafa [e,*]

[a] Department of Energy, Sumec Pakistan Private Limited, Bahawalpur, Pakistan
[b] Department of Electrical Engineering, The Islamia University of Bahawalpur, Pakistan
[c] Department of Electronic Engineering, The Islamia University of Bahawalpur, Pakistan
[d] Department of Mechatronics Engineering, Mehran University of Engineering & Technology, Jamshoro, Pakistan
[e] Department of life Sciences, University of Warwick, Coventry, United Kingdom

ARTICLE INFO

Article history:
Received 8 July 2022
Received in revised form 19 August 2022
Accepted 2 October 2022
Available online xxxx

Keywords:
Renewable energy sources
Line losses
Overloading
Voltage regulation
Power factor
Power flows

ABSTRACT

The face of state administered utility grid is suffering from a severe stress due to the rapidly growing urban communities, population, luxurious lifestyle of residents and eventually their electricity needs. This trend being accelerated at a higher pace during the past decade calls for the incorporation of alternative power sources using renewables in grid-tied or islanding mode of operation so-called microgrid. This paper addresses the technical issues associated with a 132 kV grid dedicated to Qadirpur Ran, a rural district of Pakistan located adjacent to the city of Multan. The existing electrical architecture of the district is simulated using power flow solver which illustrates that the components of the grid undergo high losses, poor voltage profile and low power factor. In addition, the simulation study identifies 20 overloaded transformers and 20 overloaded distributed lines in the existing system. Without altering the network configuration, a solar plant and a biogas plant of 10 MW capacity each along with three additional biogas plants of 5 MW (2 MW, 2 MW, 1 MW) rating which serve as emergency backup during night time are proposed for the district. As a result, the district is isolated from the national grid eliminating complexities associated with grid integration and serving as an electrically autonomous enclave. The updated hybrid system announces appealing features in a broad spectrum of electrical power framework compared to the existing quantities providing exquisite solutions to the prevailing issues. Furthermore, the cost of all-renewable powered off-grid system is calculated taking into account contributed supplementary components to estimate the total payback period of 9.75 years.

1. Introduction

The growing demand of electrical energy all over the world is an inevitable prospect enforcing the administrative authorities to step forward towards exploiting the renewable technologies. The efficient applicability of these renewable energy sources (RES) is a strategic goal to reduce dependence on fossil resources and to provide cheap, reliable and quality service to the consumers (Jarrar et al., 2020). Water pollution due to the disposal of animal and agro-industrial waste into rivers can be drastically reduced by injecting that waste for biomass energy generation to achieve sustainable development goals (SDG) (Carlini et al., 2017). Profession of agriculture and cattle farming is considered as a backbone of Pakistan's economy which holds a commendable share of ∼19% of total GDP and engages a 42% of the labor force. These hefty figures accredit rural areas of the country as dreamland to establish electrical infrastructure powered by renewable technologies such as solar and biogas.

One of the concerns associated with typical RESs (*e.g.*, solar PV and wind) is their intermittent nature since the generated electrical power is a strong function of climatic conditions such as sunshine and wind speed. Owing to the unconstrained behavior of nature beyond the human jurisdiction, hybrid operation of renewable technologies with controlled power source is assumed as a classical step towards achieving regulated supply (Sharif et al., 2017). Hybridization of RESs has highlighted its strength in terms of efficiency (Belfedhal et al., 2019), transient load fulfillment (Bajpai and Dash, 2012), cost saving (Jumare et al., 2020; Budes et al., 2017), reliability (Kekezoglu et al., 2013), long lifespan (Mishra et al., 2016) and maximizing renewable power production (Anoune et al., 2016). It is worthwhile to note that

* Corresponding author.
E-mail address: adil.mustafa@warwick.ac.uk (A. Mustafa).

https://doi.org/10.1016/j.egyr.2022.10.017

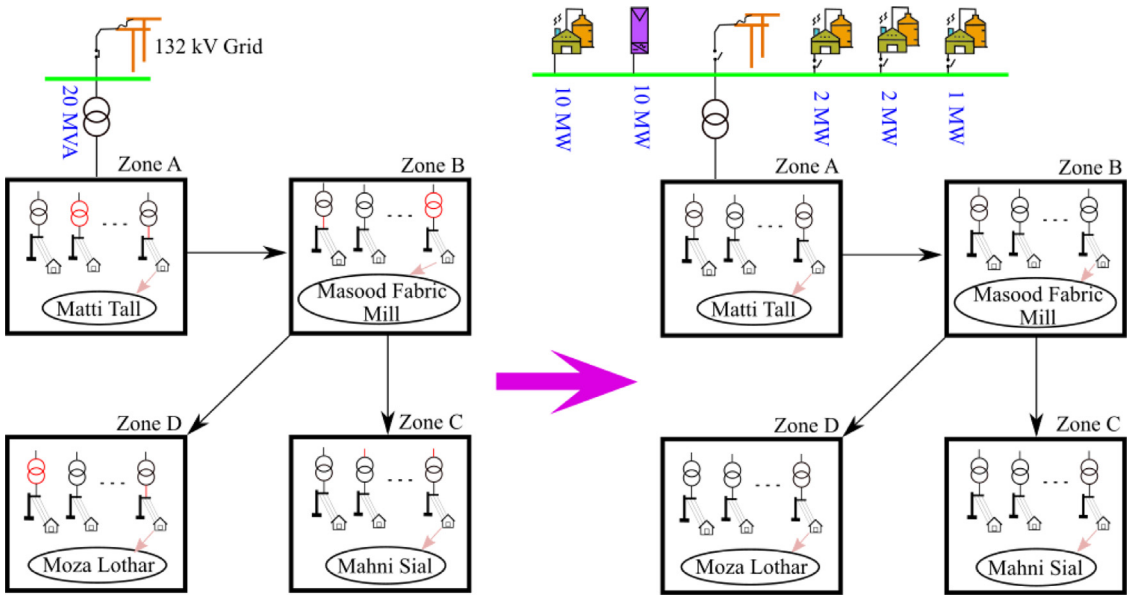

Fig. 1. Schematic diagram showing improvisation of existing 132 kV grid station in Qadirpur Ran to a hybrid off-grid network.

an intermittent source is integrated with a controlled source (*e.g.*, biogas or diesel generator) which serves as a back up in blackout or emergency situation (Sharif et al., 2017). Hybrid system runs on full potential in the context of all performance parameters subject to the expedient optimization constraints eventually leading to absolute transition from fossils to renewables (Bhandari et al., 2016).

Over the past decade, remarkable contributions have been made in the paradigm of hybrid renewable technologies to explore versatility and target shortcomings related to solitary operation. The most common selection of hybrid renewables is solar photovoltaic (solar PV) integrated with biogas plant for either centralized or distributed generation framework. Neto et al. demonstrated hybrid power system using PV modules and digesters from goat manure for sustainable rural development in the northeast semi arid region of Brazil (Neto et al., 2010). The research work was aimed to model a local cluster when it promotes the development of a whole chain of production which creates jobs and improvement to the household income in regional and rural areas. Rahman et al. presented hybrid application of solar/biomass technologies to fulfill household electricity needs in rural areas of developing countries (Rahman et al., 2014). They quantified the monetary savings and sensitivity analysis and found that a house having three to six cattle can potentially meet their cooking and electricity demands through a survey of 72 households. By replacing conventional fuel, household can save money which is more than the annual cost of installing new services as quantified using HOMER software. Later, Shahzad et al. performed techno-economic feasibility analysis of a solar/biogas off-grid system for rural electrification of Pakistan (Shahzad et al., 2017). They proposed an optimized design for an agricultural farm and a residential community centered in a village of Layyah using realistic data of solar irradiance and biomass reserves in HOMER software. In addition, they computed net present cost (NPC) and cost of electricity (COE) by performing sensitivity analysis and concluded that the proposed system is techno-economically viable.

Hybrid renewable technologies can be implemented either in grid-connected or in islanding configuration with each type having unique features and challenges. Grid connected mode of operation introduces integration issues including voltage flicker during intermittent weather, voltage rise in low demand season and harmonics from converter technologies leading to disruptions in the whole grid (Alsayegh et al., 2010). Steady operation in grid-connected mode requires management module to coordinate bidirectional flow of power between grid and hybrid RES (HRES), control of HRES, synchronization, harmonic rejection and load monitoring (Belfedhal et al., 2019). Conversely, stand alone mode of HRES provides autonomous service to the regional load center where strict conditions of integration constraints can be compromised (Aziz et al., 2020). Furthermore, off-grid configuration of HRES is solely beneficial to the local community contrary to the grid-tied scheme in which the bulk project contributes equally to the national grid.

Distributed generation using HRES has already acclaimed its incentives whose placement and ratings are evaluated by multi-objective optimization algorithms. Centralized (non distributed) generation being rather trivial approach also has the potential for improving quality of electricity apart from the economic operation; an aspect which is not comprehensively addressed so far. To cover that vacuum, this paper demonstrates implementation of a centralized generation system consisting of HRES (solar and biogas) aiming at isolating the distribution system from the grid. The study has been carried out in a small city, Qadirpur Ran, located alongside a densely populated and spacious city of Multan in southern part of Punjab province in Pakistan. The small scale renewable power plants installed in the vicinity of environmentally rich localities not only furnish local electricity needs but also provide solutions to overloading, transmission and distribution losses, poor quality and voltage regulation. The geographical location and land of agriculture nature has nominated Qadirpur Ran an endless reservoir of solar and biogas resources.

The schematic diagram of the system is shown in Fig. 1 in which the city is divided into four zones namely Zone A, Zone B, Zone C and Zone D. Zone A ranges from the grid station to a load point, Matti Tall which extends to the load center of Masood Fabric Mill in Zone B. Zone C and Zone D include the regions from Masood fabric Mill to Mahni Sial and Masood Fabric Mill to Moza Lothar respectively as shown in Fig. 1. In the first part of this research, the existing network of Qadirpur Ran is implemented in ETAP software and simulated using Newton Raphson method, a well known power flow algorithm. The details of all installed components are taken from Multan Electric Power Company (MEPCO) which is administering the concerned region and

Table 1
Load types and corresponding cost of electricity.

Load type	Maximum demand (MW)	Energy (GWh)	Unit cost (PKR/kWh)	Cost of all units (PKR)
Domestic	13.80	59.05	11.586	684,153,300
Commercial	2.22	7.60	21.14	160,664,000
Public Lighting	0.06	0.20	21.14	4,228,000
Small Industries	0.70	5.79	19.24	114,862,800
Large Industries	0.89	3.91	20.82	81,406,200
Private Tube Wells	2.33	10.205	9	91,845,000
Total	20.00	86.75	**Annual bill**	1 137 159 300

the results are computed to evaluate the state of each component and electrical performance at the user end. It is apprised that several transformers and distribution lines are overloaded which are illustrated in red colors in Fig. 1. This overloading phenomenon is mitigated by replacing all the installed transformers and lines with new components with 20% higher ratings. In the second part, a 20 MW hybrid power system consisting of biogas and solar plants of 10 MW capacity each is installed to feed different areas of Qadirpur Ran and connection to the national grid is terminated. In addition, three smaller biogas plants (2 MW, 2 MW and 1 MW) are proposed as standby alternatives in emergency situation or during night time when solar power is absent. As the comparative study suggests, the issues of high transformer and line losses, low power factor and low consumer end voltage are resolved with all the overloaded components return to the normal operating regime. In the last part, overall capital cost of the system is calculated to estimate the total payback period by considering the current electricity charges paid to the company which would be saved in all-renewable network.

This paper is organized as follows: Section 2 features some quantitative highlights of potential of solar and biogas power in Qadirpur Ran city and the characterization of the system components. Section 3 deals with simulation framework of the system in ETAP software taking into account the specifications of installed equipment and connected load units. Section 4 is dedicated to results and discussion of the system following cost analysis and payback period. Finally, the paper is concluded in Section 5.

2. Load assessment and renewable potential in Qadirpur Ran

2.1. Load demand assessment

Qadirpur Ran city is located in Multan division covering an area of ∼ 25 km^2 with a population of ∼200,000. The electric supply of the city is administered by MEPCO which has dedicated ∼20 MVA to that substation. Connected capacity does not fulfill the requirement of load for the region because of extensive power losses and low power factor. The total load of the region is categorized into domestic, commercial, industrial and tube wells whose detailed assessment is given in Table 1. The total cost of electricity is evaluated by taking into account annual energy consumption of individual unit and applying the charges for 1 unit (1 kWh) according to the government schedule.

2.2. Available solar energy resource

The geographical location of Qadirpur Ran is 30.29167°N latitude and 70.66667°E longitude and it receives a good amount of solar radiation due to its placement near equator of earth. Solar radiation data of Qadirpur Ran is obtained online from NASA Surface meteorology and Solar Energy Database (NASA surface meteorology and solar energy, 2018) and this data is given as per month average for the last 15 years *i.e.*, from Jan 2004–Dec 2018 in Fig. 2(a). The monthly average solar radiation value per day is a maximum of 6.61 kWh/m^2 in May and a minimum of 2.29 kWh/m^2 in December. The average annual solar radiation value

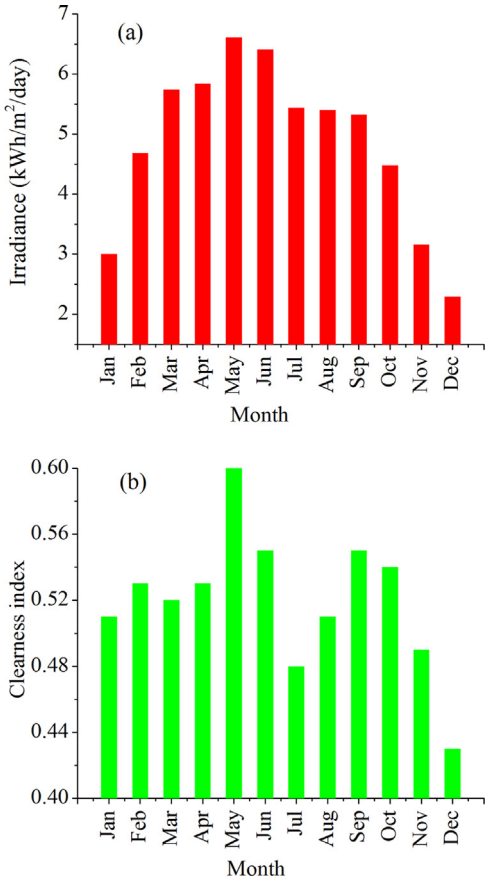

Fig. 2. Weather data of monthly averaged (a) Irradiance and (b) Clearness index at Qadirpur Ran during one year.

is 4.58 kWh/m^2. The output energy obtained by solar radiation would vary from month to month due to varying monthly solar radiation.

The clearness index (CI) defined as the fraction of radiation of solar at the top of the atmosphere that reaches a particular location on the surface of earth (Berrizbeitia et al., 2020) is plotted month wise in Fig. 2(b). Normally, CI changes from ∼0 in rainy day to ∼0.8 in the clearest condition. At Qadirpur Ran, CI value varies between a maximum of ∼0.6 in May and a minimum of ∼0.43 in December which stamps the selected site as a favorable venue for harvesting solar energy.

2.2.1. Placement of solar arrays

Aiming to gain the maximum amount of solar energy, solar panels should be positioned facing toward the sun at an angle of 90°. A two-axis solar tracker could be used to obtain maximum solar energy because the sun's position varies both seasonally and daily. The fixed slopes of solar panels are positioned towards the equator at tilt angle (β) and can be adjusted after each month.

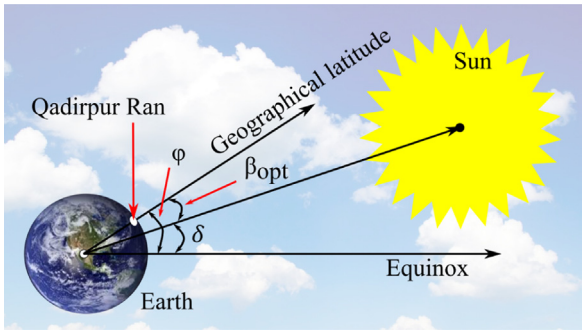

Fig. 3. Illustration of declination angle, latitude and optimum tilt angle.

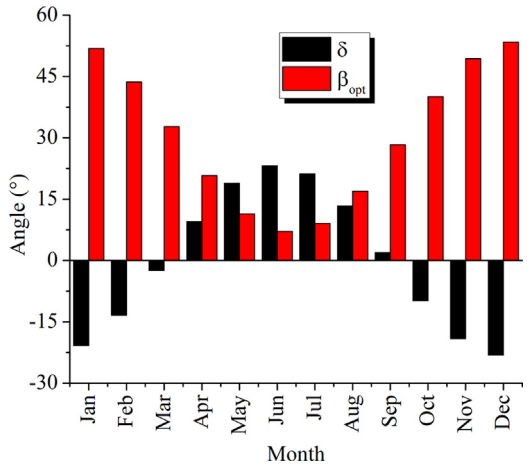

Fig. 4. Calculated declination angles and optimum tilt angles during one year.

The declination angle (δ) is the angle between the line extending from the center of the sun to the earth's center and the projection of that line on the equatorial plane of the earth (Mansouri et al., 2016). During one year, this angle varies from 23.45° during the northern hemisphere summer to −23.45° during the northern hemisphere winter (Veddeng, 2017). The declination angle can be calculated by Eq. (1) at any given day (d) of a year.

$$\delta = -23.45^\circ \times \cos\left(\frac{360}{365} \times (d + 10)\right) \tag{1}$$

Optimum tilt angle (β_{opt}) is the orientation of a solar panel at which solar radiation are incident at right angle and it depends on the geographical latitude (φ) and the declination angle (δ) as shown in Fig. 3. For that reason, it is needed to adjust the panels at β_{opt} at the instant of solar noon because solar radiation is maximum at that time. The tilt angle β_{opt} is given by the formula in Eq. (2) with all angles specified in degrees. When β_{opt} is positive, the azimuth faces south and it faces north when β_{opt} is negative. Rendering to these situations, the monthly optimal tilt angles and average declination angles for the selected area of Qadirpur Ran having latitude 30.29167°N are plotted in Fig. 4.

$$\beta_{opt} = \varphi - \delta \tag{2}$$

2.2.2. PV module specifications

In the simulation study, polycrystalline type solar panels have been considered with maximum rated power of 62.73 W, maximum power current of 3.54 A and maximum power voltage of 17.72 V. Complete detailed specification of solar module for this hybrid system is listed in Table 2.

Table 2
Parameters of solar panel (Aziz et al., 2020).

Sr. #	Parameter	Unit	Value
1.	Lifetime	years	25
2.	Derating factor	%	73.78
5.	Slope	degree	23.5
6.	Rated power (P_{MPP})	W/Panel	62.7
7.	Open circuit voltage, V_{OC}	V	22.2
8.	Short circuit current, I_{SC}	A	3.83
9.	Max. power voltage, V_{MPP}	V	17.72
10.	Max. power current, I_{MPP}	A	3.54

2.2.3. Inverter

An inverter is used to convert the DC power generated by the solar panels to AC power. Normally, the capacity of an inverter ($C_{inverter}$) is evaluated according to its efficiency and selected solar plant's power using Eq. (3):

$$C_{inverter} = P_{PV} \times 100/90 \tag{3}$$

Looking at the peak load demand, an inverter of 11.2 MW capacity is considered with an efficiency of 90% which is carefully chosen for solar plant of 10 MW output.

2.3. Biogas resource

The estimation of total electrical power generation from biogas involves the information of animal groups, total animals in each group, total volume of dung produced, fractions of dry and organic matter in the dung and specific heat in each group (Sriram and Shahidehpour, 2005). Equivalently, in this case, dung produced from the livestock of the agricultural farm during a year is calculated using Eq. (4).

$$D = \sum_{i=1}^{n} N_i.d_i \tag{4}$$

where;

D - Total animal dung per year in tons.
n - No. of specified groups of animals.
N_i - Total number of animals in group i.
d_i - Dung produced per animal in group i.

Energy of biogas (E_B) obtained from the animals' dung is estimated as given in Eq. (5) (Ofoefule et al., 2010).

$$E_B = \sum_{i=1}^{n} (N_i.d_i.k_{DM,i}.k_{OM,i}.v_{B,i}.e_{B,i}) \tag{5}$$

where:

E_B- Potential of energy obtained from the animals' dung in kWh.
e_{Bi} – Specific heat energy produced from the dung in group i in kWh/m^3.
$k_{DM,i}$ - Fraction of dry matter content in group i
$k_{OM,i}$ - Fraction of organic matter content in group i
$v_{B,i}$ - Volume of biogas per ton in group i

Electrical power (P) generated by the obtainable biogas resources is calculated as:

$$P_B = \frac{E_B}{T_c.K_e} \tag{6}$$

P_B - Electrical power generated by biogas in kW.
T_c – Plant's total operation hours throughout a year = 8760
K_e – The coefficient of electrical efficiency of the plant = 0.4

By using Eqs. (4)–(6), the manure of a total of 15 000 animals including 6000 cows, 6750 buffaloes, and 2250 others is used as biomass which is converted into biogas to generate electricity of 15 MW. Average dung produced by one animal is considered to

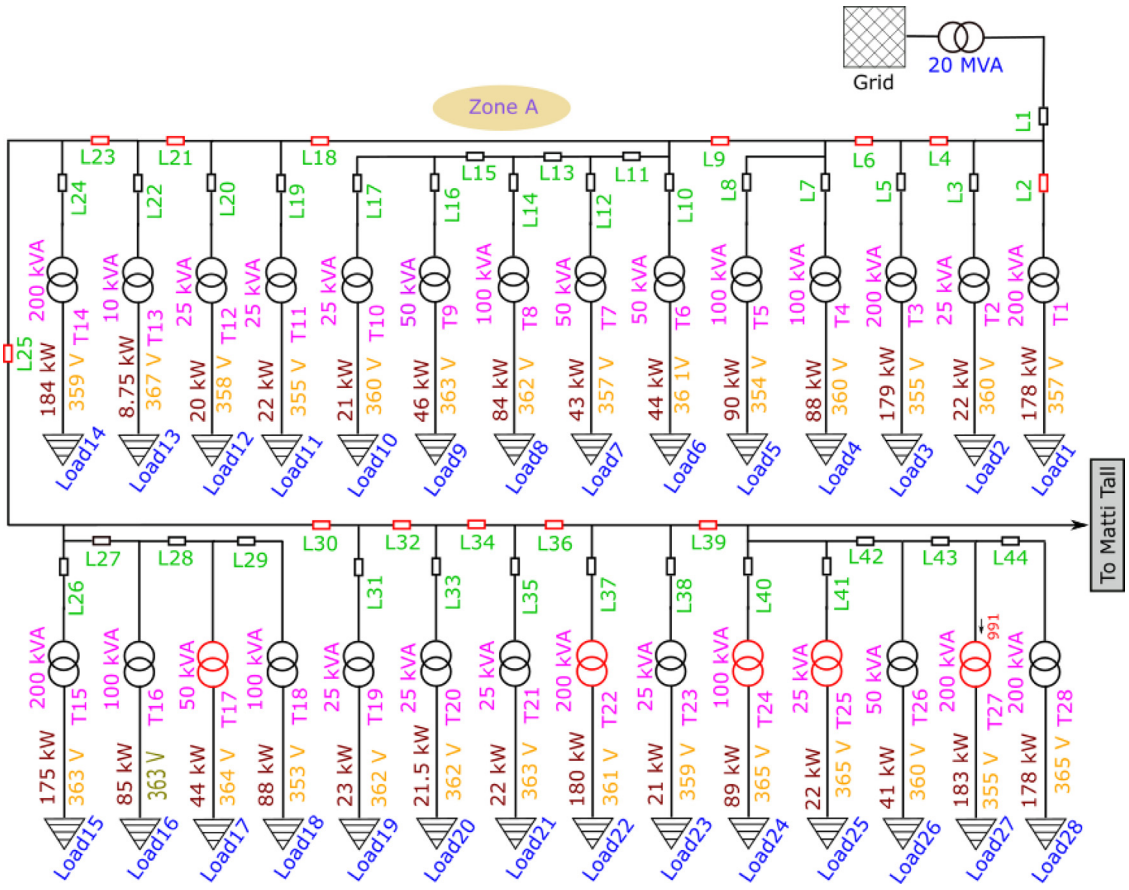

Fig. 5. ETAP simulation diagram of Zone A from grid station to Matti Tall. (For interpretation of the references to color in this figure legend, the reader is referred to the web version of this article.)

Table 3
Descriptions of animals, daily dung and resultant electrical power from biogas.

No. of animals (N)	Cows (6000)	Buffaloes (6750)	Others (2250)
Daily dung produced per head in ton (d)	0.03	0.0297	0.029
Total daily dung in ton (D)	180	182.04	65.25
Dry matter percent content (k_{DM})	0.18	0.18	0.18
Organic matter percent content (k_{OM})	0.86	0.86	0.86
Biogas output in m^3/ton (v_B)	325	320	400
Biogas heat output in kWh/m^3 (e_B)	5.8	5.8	6
Power production in MW/day (P_E)	5.85	6.50	2.65

be 29.5 kg per day throughout the year (Aziz et al., 2020). The biomass yield and production of electricity by using this data are calculated and shown in Table 3.

3. Simulation setup in ETAP

ETAP software is an exquisite simulation tool for executing power system planning, analysis and online verification protocols for dense and complicated network architectures (Zhang et al., 2020). The graphical user interface (GUI) based modeling in ETAP enables empirical foundation of an existing system opening the ways for power system engineers to upgrade an obsolete network (Rostami et al., 2020). Among other power flow algorithms, Newton Raphson method is considered to be the robust alternative due to its fast and successful convergence, less memory and computational cost (Mujtaba et al., 2020).

There are four zones to be simulated namely Zone A (Grid station to Matti Tall), Zone B (Matti Tall to Masood Fabric Mill), Zone C (Masood Fabric Mill to Mahni Sial) and Zone D (Masood Fabric Mill to Moza Lothar). Each zone is comprised of certain number of transformers, distribution lines and load centers with specific ratings and the whole system constitutes a radial network layout. Fig. 5 shows the single line diagram of Zone A of the distribution system of Qadirpur Ran district which originates from 132 kV grid followed by a 20 MVA transformer. It is worth mentioning that the first phase of simulation incorporates 132 kV grid-connected system without the installation of renewables at the high voltage bus. There are 28 transformers (T1–T28) in total in Zone A with T17, T22, T24, T25 and T27 overloaded transformers as can be seen by their red colors. Furthermore, There are 44 distribution lines (L1–L44) in total in Zone A with L2, L4, L6, L9, L18, L21, L23, L25, L30, L32, L34 and L39 overloaded distribution lines (shown in red). This status of each component is evaluated by running the simulation assuming peak load condition across each transformer. The rating of each component in the system is taken from MEPCO company manual and is labeled across as shown in Fig. 5.

Zone B of the distribution system denotes the section from Matti Tall to Masood Fabric Mill which contains total 22 transformers and 30 distribution lines as shown in Fig. 6. There are two overloaded transformers namely, T44 and T48 and six overloaded distribution lines namely, L45, L47, L51, L53, L55 and L64. The component specifications including transformer kVAs, load voltages and kWs are labeled across each entity.

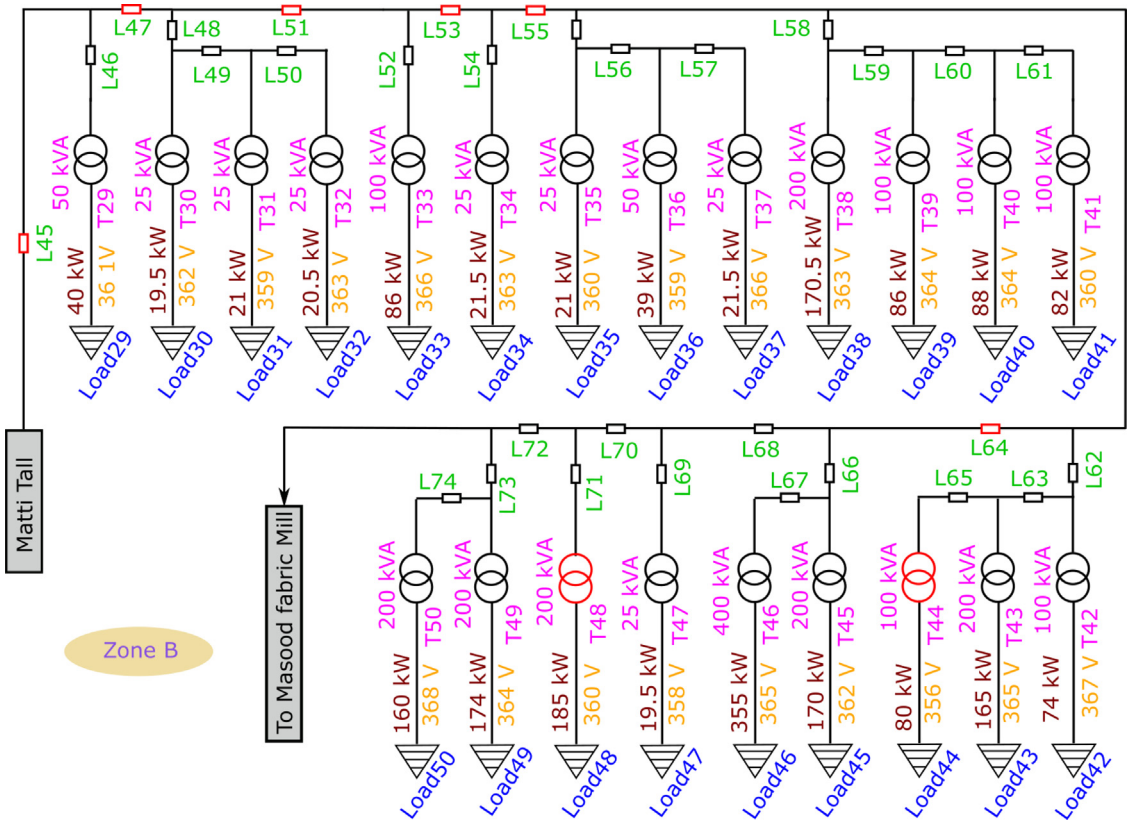

Fig. 6. ETAP simulation diagram of Zone B from Matti Tall to Masood Fabric Mill.

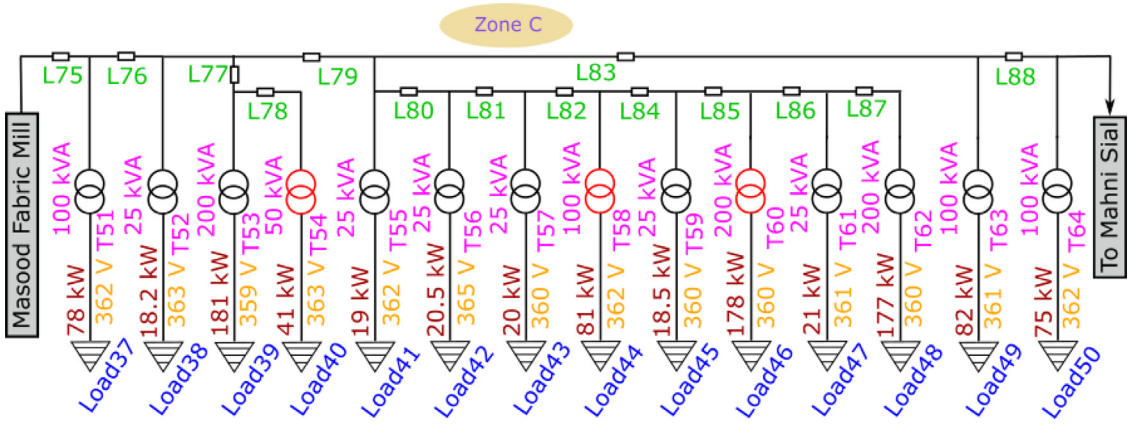

Fig. 7. ETAP simulation diagram of Zone C from Masood Fabric Mill to Mahni Sial. (For interpretation of the references to color in this figure legend, the reader is referred to the web version of this article.)

There are two regions which originate from the load center of Masood Fabric Mill namely Mahni Sial and Moza Lothar. The zone towards the load center of Mahni Sial is called Zone C which consists of 14 transformers namely T51–T64 and 14 distribution lines namely L75 to L88 as shown in Fig. 7. Three transformers highlighted in red colors are T54, T58 and T60 and there is no red distribution line identified by ETAP execution in Zone C which implies that all lines are working normally.

The section from Masood Fabric Mill to Moza Lothar is termed as Zone D which comprises 37 transformers and 47 distribution lines as shown in Fig. 8. Transformers T66, T67, T78, T80, T82, T85, T86, T91, T98 and T99 are overloaded and all distribution lines except L117 are working normally with no overloading. In the second phase of this research, all the transformers and distribution lines in the four zones are replaced with new components having 20% higher power ratings. Furthermore, the distribution system is disconnected from 132 kV national grid and a 25 MW centralized power plant of solar and biogas power is connected to the high voltage bus. As a result, the overloaded transformers and distribution lines in all the four zones return to their normal operating state which is determined by their respective black colors after executing the simulation. To save space on the paper, the entire new system with all zones is not redrawn just to show the black colors of components, nonetheless, the electrical

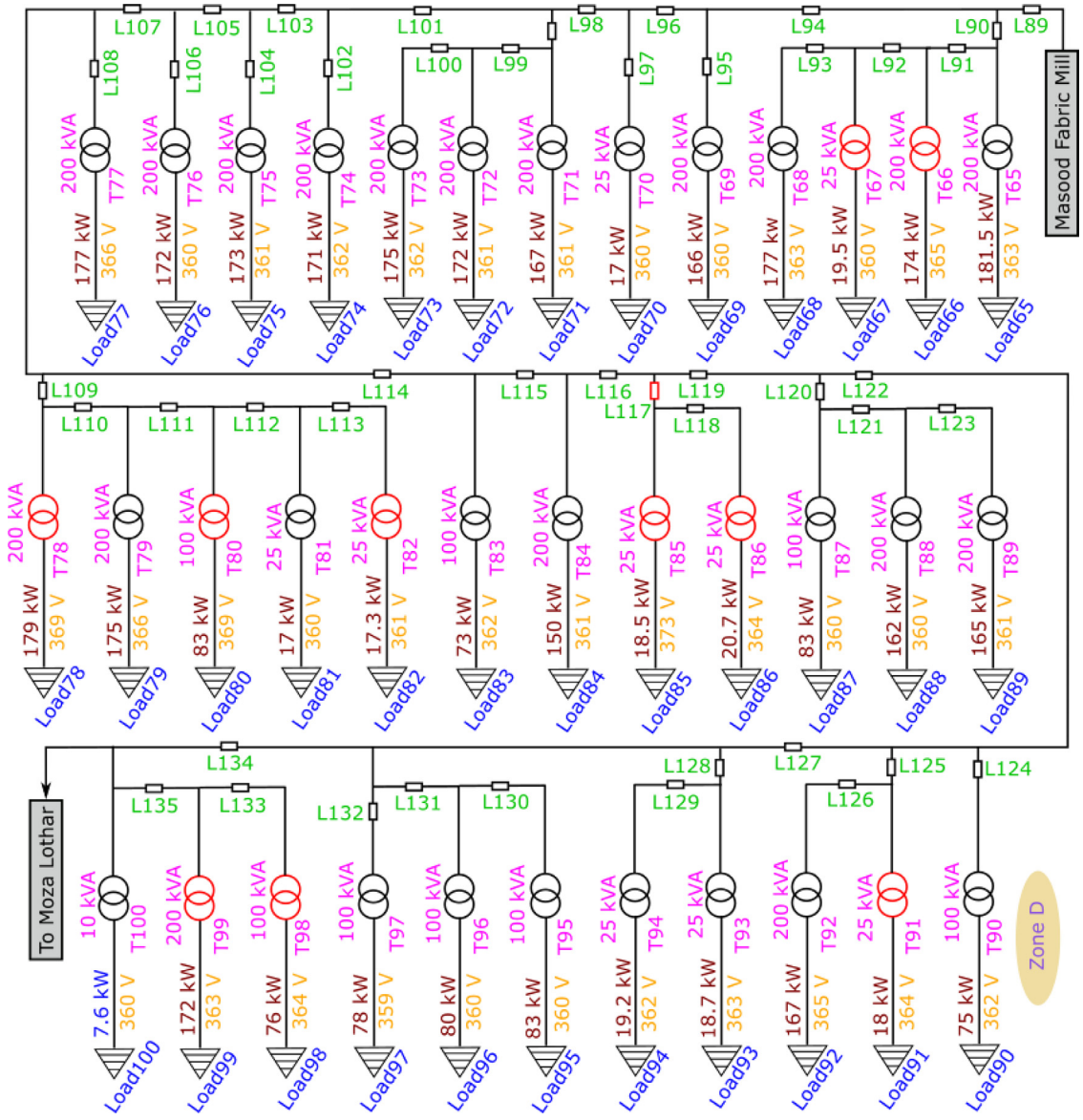

Fig. 8. ETAP simulation diagram of Zone D from Masood Fabric Mill to Moza Lothar. (For interpretation of the references to color in this figure legend, the reader is referred to the web version of this article.)

outputs at the loads and losses across all components are plotted in the next section both for the existing and hybrid systems.

4. Results and discussion

This section deals with the comparison of transformer losses, line losses, power factor and voltage profile across the components in all the zones of the distribution system. It is apprised that the existing system is being fed by the utility grid and it is subjected to behave differently when connected to a dedicated high voltage bus of renewables. The existing national grid is experiencing harsh backlash due to a remarkable gap between generation and consumption of both active and reactive powers in the distribution network. The quality of supply at the consumer side is prone to deteriorate causing unscheduled blackouts, power system faults, component tripping/failure, expensive tariffs and several financial penalties. The underlying quantities defining the power system performance include losses, power factor and voltage regulation at each bus whose explanation is provided in the next subsections.

4.1. Transformer losses

The equivalent circuit of transformer is reactive in nature due to the presence of windings making up the magnetization and leakage inductance which absorb the reactive power supplied by the generators. In order to minimize magnetic losses which are attributed to leakage inductance of winding, equivalent reactive power must be supplied by the generators to compensate the inductive reactance and cancel out the leakage flux. In case of overloaded grid, required active and reactive powers are not supplied by the set of generators therefore, the transformers are also overloaded and produce magnetic losses. The proposed hybrid system has satisfactory rating to produce both power

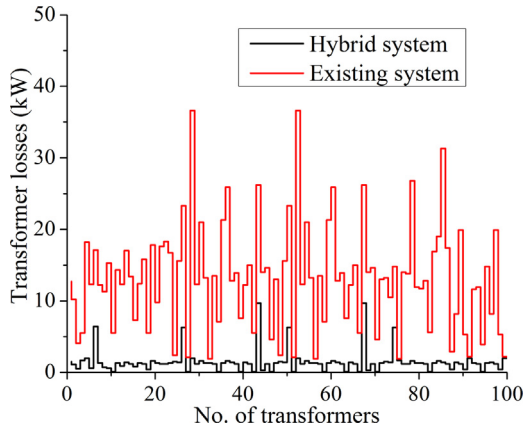

Fig. 9. Comparison of transformer losses of existing system and new off-gird hybrid system.

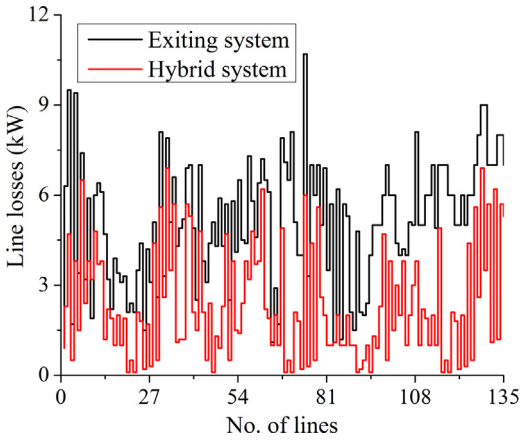

Fig. 10. Comparison of line losses of existing system and new off-grid hybrid system.

components and restore the operating conditions and in addition, the overloading issue of transformers is eliminated by increasing their ratings up to 20%.

There are in total 100 transformers in the distribution system and losses across each entity are plotted in Fig. 9. In the existing system, minimum transformer losses of 1.9 kW occur across T33 while losses are quite high across most of the transformers with a maximum value of 36.6 kW across T29. On the other hand, in solar/biogas hybrid system, minimum losses of 0.1 kW occur across many transformers and maximum losses of 9.7 kW occur across T68. The transformer loss is an important prospect in a power system to ensure efficiency and stability of the overall system. Clearly, hybrid system possesses much smaller transformer losses compared to the existing counterpart as a result of increased generation and transformer rating to furnish enhanced stability of supply to the consumers.

4.2. Line losses

The power losses across distribution lines is attributed to the ohmic drop in their resistive circuit which causes increased temperature rise, degradation of insulation jackets and in turn their life time. It is notable that most of the household loads which are closed loop systems namely air conditioners, room heaters, water heaters and refrigerators work on constant power principle. When sufficient reactive power is not supplied by the generator, system voltage drops and such regulating loads draw more current to maintain the power and the reference variable *e.g.* temperature. As a result of excessive current, line losses increase and the second cause of this increase is the smaller rating or diameter of the conductor causing higher resistance.

Line losses in the distribution system in turn deteriorate the efficiency by a considerable factor resulting into poor quality of supply and low voltage to the end user. In the existing system, minimum line losses of 1 kW occur across L1 and maximum line losses occur across L75 with a value of 10.7 kW. In the solar/biogas hybrid system, cable losses are minimum and maximum across L91 and L129 with values of 0.1 kW and 6.9 kW respectively as shown in Fig. 10. Clearly, copper losses are reduced drastically in hybrid system compared to the existing system as a result of more injected power from HRES as well as higher rating of the lines.

4.3. Power factor

Low power factor at the consumer side causes higher current drawn by the equipment at load to supply the required

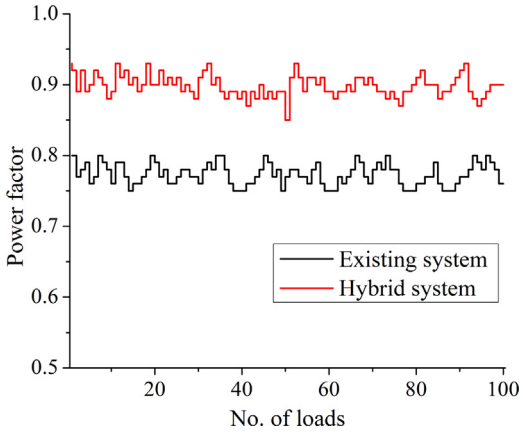

Fig. 11. Load power factor comparison before and after installing new solar/biogas distributed generation system.

reactive current resulting into higher transmission capacity and higher losses. The underlying idea behind low power factor is the generation of unequal reactive power as required by the load due to which an oscillatory current constantly flows through the network. For an already overloaded national bus, the deficiency of reactive power degrades the network power factor so the overall throughput and utilization factor of the system decreases.

The power factor across all the load units from Load1 to Load100 are plotted in Fig. 11. In the existing system, power factor ranges from 0.75 to 0.80 and these extreme values occur across several load units. In hybrid system, minimum power factor is 0.87 and maximum value is 0.93 and these values are much higher compared to those in the existing system. Copper losses in the system also increase due to the low power factor. New power factor is close to unity which is a good sign for low current, low copper losses and a healthy system. Improved power factor also reduces the equipment's economic cost because the current is reduced.

4.4. Receiving end voltage

The final correlated network parameter is the bus voltage which is also a strong function of losses, reactive power and power factor across each component. Whenever, there is a deficiency of active and/or reactive power generation compared to the load demand, voltage drops which not only affects the load appliances but also disturbs the other operating variables.

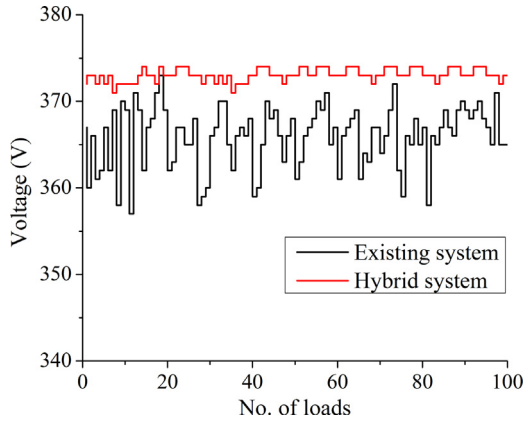

Fig. 12. Comparison of receiving end voltages before and after analysis.

The final part of this section deals with the investigation of receiving end voltage across Load1 to Load100 for the existing and hybrid systems as shown in Fig. 12. In the existing system, minimum receiving end voltage is recorded as 357 V across Load12 and a maximum value of 373 V is observed at Load19. In solar/biogas hybrid system, receiving end voltages vary from 371 V to 374 V which are quite higher than those in the existing system and close to the nominal receiving end line to line voltage which is 380 V. The voltage regulation is an unwanted phenomenon which results into anomalous behavior including heating up of the modern sophisticated appliances and reducing their life times.

4.5. Cost analysis and payback period

The analysis of the cost of a million dollar venture is an essential exercise even after the acceptance of the technical feasibility of the proposed system. For this project, it is apprised that the cost of electricity charged from the consumers will remain same whose tariffs are summarized in Table 1. Needless to say that the hybrid solar/biogas system is purely autonomous with 100% natural resources collected from the local society. Therefore, apart from the initial installation costs (IC) of the plants, the system requires operation and maintenance charges (OMC) including labor, repair, routine cleaning and tuning of the equipment (Gurturk, 2019). In the first part, the installation cost of the solar plant is estimated from the "US Solar Photovoltaic System Cost Benchmark" manual published by National Renewable Energy Laboratory (NREL) which reports the average cost in dollars per watt (Fu et al., 2018). The gross cost of solar installation per watt has reduced drastically over the years and it is 1.13 $/W in 2018. Assuming 1$ = 160 PKR which is the current currency rate and upscaling the cost for 10 MW, the total investment cost (IC_s) for 10 MW solar plant is calculated. Similarly, the annual operation and maintenance cost of solar plant (OMC_s) is 14 $/kW/Y which is converted to PKR/10 MW/Y to account for the 10 MW power generation.

The installation cost to produce electrical energy of 7.5 GWh/Y (equivalent to 0.85 MW) from biogas plant is 2.5 M$ as demonstrated by a technical report from Winrock International (Subedi, 2013). For the current project of 15 MW, the amount for IC_b converted to PKR is recalculated along with the OMC_b in PKR/15 MW/Y. As stated before, the cost of electricity charged from the consumers (Annual bill) is same which is summarized in Table 1, the annual saving is calculated by subtracting the OMC of both plants from the Annual bill as shown in Eq. (7).

$$\text{Annual saving} = \text{Annual bill} - OMC_s - OMC_b \tag{7}$$

Table 4
Descriptions and numerical values of cost parameters.

Sr. #	Parameter description	Value
1	IC_s ($/W)	1.13
2	IC_s (PKR/10 MW)	1 808 000 000
3	OMC_s ($/kW/Y)	14
4	OMC_s (PKR/10 MW/Y)	22 400 000
5	IC_b ($/0.85 MW)	2.5×10^6
6	IC_b (PKR/15 MW)	7 008 000 000
7	OMC_b (PKR/15 MW/Y)	210 240 000
8	Annual bill (PKR/Y)	1 137 159 300
9	Annual saving (PKR/Y)	904 519 300
10	Payback period (Y)	9.75

Finally, the payback period in years is calculated by dividing the total installation cost (IC) by annual saving which is calculated to be 9.75 years or 09/10/19 (YY/MM/DD) as shown in Eq. (8).

$$\text{Payback period} = \frac{IC_s + IC_b}{\text{Annual saving}} \tag{8}$$

The resultant quantities of costs of both plants, annual bill, annual savings and payback period of the whole system is summarized in Table 4.

5. Conclusion

This paper presented an improvisation scheme of an existing 132 kV grid of Qadirpur Ran, a rural area located adjacent to Multan in southern part of Punjab, Pakistan. A survey was conducted to obtain the total load, network layout, annual bill and specifications of transformers and distribution lines from MEPCO to implement the system in ETAP. Subsequently, the simulation was executed to analyze the system behavior at the consumer end along with the health of intermediate components. There were 20 transformers and 20 distribution lines which were observed to be overloaded after the power flow execution due to which the overall system is electrically unstable and ill-planned. This has caused poor voltage profile, low power factor and high transformer and copper losses further amplifying the extent of improficiency of the service.

The solutions to these overwhelming issues were addressed by increasing the ratings of all installed transformers and distribution lines by 20% in the simulation setup. Furthermore, the distribution system was disconnected from 132 kV national grid and was fed by a solar plant of 10 MW capacity along with four biogas plants of 15 MW capacity in total in compliance to the demand. The comparison of simulation results of upgraded system with those of the existing system reveals that all transformers and distribution lines are operating in normal conditions without overloading. Consequently, transformer losses, copper losses are reduced remarkably compared to the existing system case. The voltage profile and power factors across each load unit also come closer to the nominal/ideal values in the hybrid system with better component ratings.

In the final part, cost analysis was carried out to estimate the total expenditures in the installation of the hybrid system and annual running expenses required for operation and maintenance. Assuming same billing rates were charged from the consumers as were done by MEPCO, annual bill was calculated out of which annual operation and maintenance charges were subtracted to calculate total annual savings. The calculated annual saving represented a duration of approximately 9.75 years which would be required to fully payback the installation cost of the hybrid system. The proposed quantitative analysis along with the feasibility report authenticates the profitability of this multibillion project and its certain revenue return.

CRediT authorship contribution statement

Muhammad Imran: Conceptualization, Methodology, Software. **Zeeshan Rashid:** Data curation, Writing – original draft, Project administration, Supervision. **Muhammad Amjad:** Visualization, Investigation, Resources. **Shadi Khan Baloch:** Formal analysis, Writing – review & editing. **Adil Mustafa:** Supervision, Validation, Funding acquisition.

Declaration of competing interest

The authors declare that they have no known competing financial interests or personal relationships that could have appeared to influence the work reported in this paper.

Data availability

The data used in the research work is provided in the manuscript

Acknowledgments

This work is supported by University of Warwick, United Kingdom under the Research Excellence Framework exercise – REF-after-REF2021.

References

Alsayegh, O., Alhajraf, S., Albusairi, H., 2010. Grid-connected renewable energy source systems: Challenges and proposed management schemes. Energy Convers. Manage. 51 (8), 1690–1693.

Anoune, K., Bouya, M., Ghazouani, M., Astito, A., Abdellah, A.B., 2016. Hybrid renewable energy system to maximize the electrical power production. In: 2016 International Renewable and Sustainable Energy Conference. IRSEC, Marrakech, Morocco, pp. 533–539.

Aziz, M.S., Khan, M.A., Khan, A., Nawaz, F., Imran, M., Siddique, A., 2020. Rural electrification through an optimized off-grid microgrid based on biogas, solar, and hydro power. In: 2020 International Conference on Engineering and Emerging Technologies. ICEET, Lahore, Pakistan, pp. 1–5.

Bajpai, P., Dash, V., 2012. Hybrid renewable energy systems for power generation in stand-alone applications: A review. Renew. Sustain. Energy Rev. 16 (5), 2926–2939.

Belfedhal, S.A., Berkouk, E.M., Messlem, Y., 2019. Analysis of grid connected hybrid renewable energy system. J. Renew. Sustain. Energy 11, 014702.

Berrizbeitia, S.E., Gago, E.J., Muneer, T., 2020. Empirical models for the estimation of solar sky-diffuse radiation. A review and experimental analysis. Energies 13 (3), 701.

Bhandari, B., Ahn, S.-H., Ahn, T.-B., 2016. Optimization of hybrid renewable energy power system for remote installations: Case studies for mountain and island. Int. J. Precis. Eng. Manuf. 17 (6), 815–822.

Budes, F.B., Ochoa, G.V., Escorcia, Y.C., 2017. Hybrid PV and wind grid-connected renewable energy system to reduce the gas emission and operation cost. Contemp. Eng. Sci. 10 (26), 1269–1278.

Carlini, M., Mosconi, E.M., Castellucci, S., Villarini, M., Colantoni, A., 2017. An economical evaluation of anaerobic digestion plants fed with organic agro-industrial waste. Energies 10 (8), 1–15.

Fu, R., Feldman, D., Margolis, R., 2018. U.S. solar photovoltaic system cost benchmark.

Gurturk, M., 2019. Economic feasibility of solar power plants based on PV module with levelized cost analysis. Energy 171, 866–878.

Jarrar, L., Ayadi, O., Asfar, J.A., 2020. Techno-economic aspects of electricity generation from a farm based biogas plant. J. Sustain. Develop. Energy, Water Environ. Syst. 8 (3), 476–492.

Jumare, I.A., Bhandari, R., Zerga, A., 2020. Assessment of a decentralized grid-connected photovoltaic (PV) / wind / biogas hybrid power system in northern Nigeria. Energy, Sustain. Soc. 10 (30), 1–25.

Kekezoglu, B., Arikan, O., Erduman, A., Isen, E., Durusu, A., Bozkurt, A., 2013. Reliability analysis of hybrid energy systems: Case study of Davutpasa campus. In: Eurocon 2013. IEEE, Zagreb, Croatia, pp. 1141–1144.

Mansouri, E., Pirsalami, M.H., Nasiri, N., Farrizi, M., Hashemizadeh, M., Alihosseini, H., 2016. Optimum tilt angle for fixed-array solar panels at a constant latitude of 29 to receive the maximum sunlight. Bull. Environ. Pharmacol. Life Sci. 26 (1), 26–30.

Mishra, S., Panigrahi, C., Kothari, D., 2016. Design and simulation of a solar–wind–biogas hybrid system architecture using HOMER in India. Int. J. Ambient Energy 37 (2), 184–191.

Mujtaba, G., Rashid, Z., Umer, F., Baloch, S.K., Hussain, G.A., Haider, M.U., 2020. Implementation of distributed generation with solar plants in a 132 kV grid station at Layyah using ETAP. Int. J. Photoenergy 2020, 1–14.

NASA surface meteorology and solar energy. Global/regional data. http://www.eso.org/gen-fac/pubs/astclim/espas/world/Climate/ITCZ/ION/ion-pwv.html, NASA Langley Research Center Hampton, VA United States.

Neto, M.B., Carvalho, P., Carioca, J., Canafistula, F., 2010. Biogas/photovoltaic hybrid power system for decentralized energy supply of rural areas. Energy Policy 38 (8), 4497–4506.

Ofoefule, A.U., Nwankwo, J.I., Ibeto, C.N., 2010. Biogas production from paper waste and its blend with cow dung. Adv. Appl. Sci. Res. 1 (2), 1–8.

Rahman, M.M., Hasan, M.M., Paatero, J.V., Lahdelma, R., 2014. Hybrid application of biogas and solar resources to fulfill household energy needs: A potentially viable option in rural areas of developing countries. Renew. Energy 68 (3), 35–45.

Rostami, A., Mohammadi, M., Rastegar, M., 2020. An improved transformation based probabilistic load flow analysis using appropriate reference variable. Int. J. Electr. Power Energy Syst. 120, 106052.

Shahzad, M.K., Zahid, A., Rashid, T.U., Rehan, M.A., Ali, M., Ahmad, M., 2017. Techno-economic feasibility analysis of a solar-biomass off grid system for the electrification of remote rural areas in Pakistan using HOMER software. Renew. Energy 106, 264–273.

Sharif, M.S.E., Khan, M.M.Z., Moniruzzaman, M., Bose, A., 2017. Design, simulation and stability analysis of wind-PV-diesel hybrid power system using ETAP. Amer. J. Modern Energy 3 (6), 121–130.

Sriram, N., Shahidehpour, M., 2005. Renewable biomass energy. In: IEEE Power Engineering Society General Meeting, 2005. San Francisco, CA, USA, pp. 612–617.

Subedi, P.S., 2013. Medium sized biogas plants: Pakistani experiences and regional prospects.

Veddeng, I., 2017. Techno-economic analysis of hybrid solar PV and bioenergy system for use in rural areas of Myanmar (M.Sc. thesis). Norwegian University of Life Sciences.

Zhang, Z., Kang, Y., Xie, X., 2020. Online verification method of relay protection settings based on etap software. In: IOP Conference Series: Earth and Environmental Science, Vol. 514. (4).